Monte Carlo simulations of the rate of intramolecular end-to-end contact in alkane chains

J. A. Nairn[a] and C. L. Braun

Department of Chemistry, Dartmouth College, Hanover, New Hampshire 03755
(Received 22 August 1980; accepted 15 October 1980)

We report Monte Carlo simulations of the dynamics of intramolecular contact in alkane chains and in end-labeled alkane chains. The chain is confined to a diamond lattice except during conformational jumps. Rotational jumps around internal bonds provide the mechanism for change in the end-to-end separation but crankshaft-like motions of the chain are also permitted. No adjustable parameters are used. End-to-end contact is found to obey first-order kinetics, and the rate constants for contact decrease monotonically with chain lengths of from 10 to 20 atoms. Simulations for end-labeled chains are compared with experimental measurements of intramolecular electron transfer and intramolecular fluorescence quenching.

I. INTRODUCTION

In the classic problem of the probability of ring formation by a chain with reactive end groups, the equilibrium distribution of chain conformations governs the results obtained unless the cyclization reaction occurs with high probability upon first contact of the reactive groups.[1-11] Literature examples of cyclization reactions seem all to fall in the low reaction probability limit in which the equilibrium distribution of conformations[8] is little perturbed by chemical reaction. However, in an earlier paper, Nairn *et al.*[12] reported an example of intramolecular fluorescence quenching that does appear to occur on every end-to-end contact and whose rate thus reflects the chain dynamics. The technique developed here will be used to simulate those and several related experiments.

We formulate a Monte Carlo approach to the estimation of the rate constants for end-to-end contact in *n*-alkane chains of 10 to 20 carbons and evaluate the characteristic time for a chain conformation selected from among the equilibrium distribution to evolve until the chain ends come into contact. We are thus concerned both with simulation of equilibrium conformational distributions and with the rates of change of one chain conformation into another.

The rotational isomeric state (RIS) model provides a powerful approach to the understanding of the equilibrium distribution of chain conformations.[13] Specifically, for short chains, Winnik has recently reviewed experimental and theoretical approaches to the study of equilibrium conformational distributions,[14] which he has probed by measurement of rate constants for intramolecular hydrogen abstraction by an excited chromophore attached to a chain end. For alkane chains of from 10 to 22 carbons, he finds excellent agreement between the measured rates and theoretical predictions based on a diamond-lattice model of the equilibrium conformations.[15]

We too confine the carbon backbone of the chains we examine to a diamond lattice. In this simplified form of the RIS model for alkane conformations,[8] all C–C bond distances are fixed at 1.53 Å and C–C–C bond angles are taken to be 109.5°. Rotational dihedral angles are limited to $\phi = 0$ (*trans*, *t*), $\phi = +120$ (*gauche*, g^+), or $\phi = -120$ (*gauche* minus, g^-).

In our simulations of the rate of end-to-end contact in short chains, a diamond-lattice conformation is first generated by a Monte Carlo method similar to that described by Fixman and Alben.[8] The initial conformation is then subjected to a series of random-number-determined bond motions which have the eventual effect of bringing the two chain ends to within some prescribed "contact" separation. The time taken for evolution of the initial conformation into a contacting conformation is computed by multiplying the number of bond jumps required to achieve contact by the mean time for a jump, which is separately computed. Repetition of the proceduce is used to generate a histogram of the number of surviving (i.e., not yet in end-to-end contact) chains versus time. The number of surviving chains is found to decay approximately exponentially. Thus, a least squares fit to a histogram of the logarithm of the number of surviving chains versus time yields a first-order rate constant for intramolecular end-to-end contact which may be compared with experiment. It may be remarked that our model invokes no adjustable parameters.

The description of the simulations is organized into the following sections: (1) Monte Carlo simulation of equilibrium chain conformations; (2) description of allowed motions; (3) real elapsed time versus the number of successful timed jumps; and (4) results of simulations of the end-to-end contact rates of short *n*-alkanes, of intramolecular fluorescence quenching, and of electron transfer between groups attached at the chain ends.

II. THE MODEL

As described in the Introduction, the computer modeling begins with the generation by the RIS approach[15] of a single chain conformation. Conformations are chosen by considering nearest neighbor interactions which determine that the conformation about bond i (ϕ_i) depends on the conformation about bond $i-1$ (ϕ_{i-1}). The statistical weight for a rotational angle ϕ_i at bond i is $U(\phi_{i-1},$

[a]Present address: Laboratory of Chemical Biodynamics, Lawrence Berkeley Laboratory, University of California, Berkeley, Cal. 94720.

 0021-9606/81/042441-09$01.00

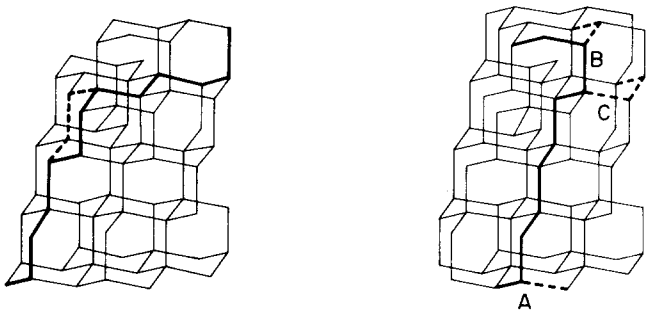

FIG. 1. Motions on a diamond lattice. *A* is rotation of a methyl group, *B* is rotation of an ethyl group, and *C* is rotation of a propyl group.

$\phi_i) = \exp(-E(\phi_{i-1}, \phi_i)/RT)$, where $E(\phi_{i-1}, \phi_i)$ represents the relative energy of the nearest neighbor interactions. The statistical weights can conveniently be written as elements of a 3×3 matrix $U(\phi_{i-1}, \phi_i) = U_{kl}$, where the indices 1, 2, and 3 correspond to t, g^+, and g^-, respectively. The resulting matrix is[8]

$$U = \begin{pmatrix} 1 & \sigma & \sigma \\ 1 & \sigma & \sigma\omega \\ 1 & \sigma\omega & \sigma \end{pmatrix} , \tag{1}$$

where $\sigma = \exp(-500\ \text{cal}/RT)$ and $\omega = \exp(-2000\ \text{cal}/RT)$.[15] At 300 K, $\sigma = 0.43$ and $\omega = 0.035$. Throughout the simulations, we neglect long-range excluded volume effects.

A. Allowed motions

Once selected, a random chain is subjected to a series of internal motions until the ends come within a specified contact separation. For a diamond-lattice chain, the only types of motion which bring about changes in the end-to-end distance are rotations of end groups of the chain (ethyl, propyl, butyl, etc.) about bonds (see Fig. 1). A rotation about bond i in an RIS chain can be simply described as a jump in which the conformation about bond i changes ($g^+ \rightarrow g^-$, $g^+ \rightarrow t$, $t \rightarrow g^+$, etc.) while the conformations about all other bonds remain the same. Rotations about terminal bonds do not change the chain conformation and can be ignored. Rotations about bonds 2, 3, 4, etc. are incorporated in the model. Because of frictional interactions with solvent, the rate constant for a rotational transition about an internal bond is expected to decrease as the end group which rotates increases in length.

A chain segment is also permitted to undergo a three-bond jump[16] which can be visualized as the crankshaft motion of three bonds from one side of a cyclohexane chair conformation to the other side (see Fig. 1). A three-bond jump is only possible if the central bond is g^+ or g^- and not part of a g^+g^- sequence. The net effect of the jump is to convert a central bond that is g^+ to g^- or *vice versa*. Three-bond jumps do not change the end-to-end distance. Despite this fact, their potentially important role in modeling the rate of end-to-end contact is to facilitate diffusion of conformational changes along the chain.[16]

B. Execution of allowed motions

The type of attempted motion is determined by the choice of a random number between 0 and Z, where

$$Z = \sum_{i=2}^{n-1} ({}^iw_3 + {}^iw_r) . \tag{2}$$

Here ${}^iw_3$ is a weight that is proportional to the probability of attempting a three-bond jump at bond i, ${}^iw_r$ is a weight that is proportional to the probability of attempting a rotation about bond i, and the sum is over the internal bonds of the chain. Each type of motion is assigned a portion of the 0 to Z random number space equal to its weight. Because the probability for attempting a three-bond jump is expected to be independent of i, we take all ${}^iw_3$ equal and scale the random number space so that ${}^iw_3 = 1$. Thus,

$$Z = n - 2 + \sum_{i=2}^{n-1} {}^iw_r . \tag{3}$$

If the randomly selected motion is a three-bond jump about a central bond that is in a t state or part of a g^+g^- configuration, no jump is possible and the attempted motion is unsuccessful. To retain physical significance in the model, the probability of *successful* three-bond jumps, and not of *attempted* three-bond jumps, should be proportional to the actual rate constant $1/\tau_3$ for a three-bond jump. We therefore introduce a term S_3 which gives the average probability that a three-bond jump is successful given that a three-bond jump is attempted. We write

$$S_3 = K/\tau_3 , \tag{4}$$

where τ_3 is the jump time (reciprocal first-order rate constant) for a three-bond jump and K is a constant. Averaging over internal bonds

$$S_3 = \frac{1}{n-2} \sum_{i=2}^{n-1} 2[P_{i-1}(t)\sigma + P_{i-1}(g^+)\sigma - P_i(g^+)\sigma\omega] , \tag{5}$$

where $P_{i-1}(t)$ and $P_{i-1}(g^+)$ are the probabilities that bond $i-1$ is t and g^+, respectively. The summand is just the probability that bond i is g^+ or g^- but not part of a g^+g^- configuration, i.e., the probability that a three-bond jump is possible. $P_i(t)$ and $P_i(g^+)$ can easily be found from the elements of the powers of U, namely,

$$P_i(t) = (U^{i-1})_{11} , \tag{6}$$

$$P_i(g^+) = (U^{i-1})_{12} . \tag{7}$$

At 300 K, we find that S_3 is 0.40.

Because we allow chain intersections, rotation about any selected bond is always conceivable. To a first approximation, the rotation rate about bond i depends on the change in configuration of bond i. Recall that g^+ and g^- are 500 cal above t (see Fig. 2). Thus, from microscopic reversibility, the ratio of the jump time $\tau_{g\rightarrow t}$ for a rotation that changes the conformation of a bond from $g \rightarrow t$ to the jump time $\tau_{t\rightarrow g}$ for a rotation that changes the conformation of a bond from $t \rightarrow g$ is

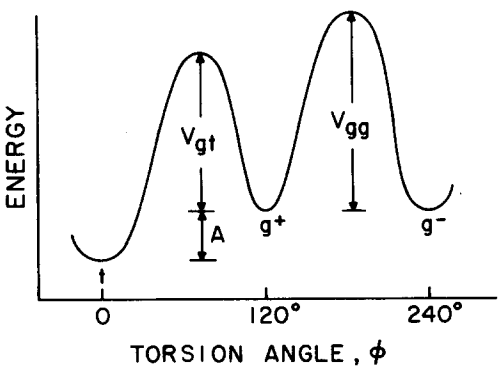

FIG. 2. Reaction coordinate diagram for rotations about a bond. The energy difference A is taken to be 500 cal/mol (see Ref. 13).

$$\tau_{g^+t}/\tau_{t^-g^-}=\sigma \ . \tag{8}$$

Similarly,

$$\frac{\tau_{g^-t}}{\tau_{g^+g^-}}=\exp[-(V_{gg}-V_{gt})/RT]=\sigma' \ , \tag{9}$$

where V_{gg} and V_{gt} are defined in Fig. 2 and $\tau_{g^+g^-}=\tau_{g^-g^+}$. (In most of our simulations we used $V_{gg}=V_{gt}$; the implications of this assumption are considered in the Discussion.)

Consider a bond which is g^+ (or g^-). A rotation about this bond will change its configuration to t with a jump time τ_{g^+t} and to g^- (g^+) with a jump time $\tau_{g^+g^-}$. Thus, a bond that is g^+ rotates with a jump time τ_{g^+}, where

$$\frac{1}{\tau_{g^+}}=\frac{1}{\tau_{g^+t}}+\frac{1}{\tau_{g^+g^-}} \ . \tag{10}$$

The rotation will go to a t state with probability τ_{g^+}/τ_{g^+t} and to a g^- state with probability $\tau_g/\tau_{g^+g^-}$. Analogously, a bond that is t rotates with a jump time τ_{t^-} given by

$$\frac{1}{\tau_{t^-}}=\frac{2}{\tau_{t^-g}} \ . \tag{11}$$

To allow rotations to occur with the correct probability, we used the following scheme: The weights ${}^iw_r$ are determined by the rate constant for rotation out of a g state at bond i, i.e., ${}^iw_r$ is proportional to $1/\tau_{g^-}$. Because the proportionality constant is equal to K in Eq. (4),

$${}^iw_r=S_3\tau_3/{}^i\tau_{g^-} \ . \tag{12}$$

If the selected motion is a rotation about a bond that is g^+ (or g^-), the rotation always occurs and selection of a second random number causes the final state to be t or $g^-(g^+)$ according to the probabilities defined in the preceding paragraph. If the motion selected is rotation about a bond that is t, a rotation occurs with only the probability τ_{g^-}/τ_{t^-}. Such rotations result in g^+ or g^- states with equal probability.

Thus far, we have neglected the effect of g^+g^- sequences. Because such sequences are energetically disfavored, rotations out of g^+g^- states should be extremely fast. We treat such rotations in the following manner: (1) If the selected motion is a rotation about a bond that is part of a g^+g^- sequence, the rotation occurs but the timing counter (*vida infra*) is not incremented, i.e., the rotation is instantaneous. (2) If after any rotation the selected bond is found to be part of a g^+g^- sequence, a second rotation occurs without incrementing the timing counter.

C. Timing

The time T for the two ends to come into contact is proportional to the number of successful jumps which is counted by the timing counter j. The proportionality constant relating T and j is equal to the average time between j-incrementing jumps anywhere on the chain. This average time is equal to τ_3 times the number of successful three-bond jumps about a particular bond per j-incrementing jump anywhere on the chain. Thus, we have

$$T=\frac{S_3\tau_3}{ZQ}j \ , \tag{13}$$

where S_3/Z is the probability of a successful three-bond jump around a particular bond and Q is the average probability that any attempted jump results in a j-incrementing jump. Averaging over all internal bonds,

$$Q=\frac{1}{Z}\sum_{i=2}^{n-1}(S_3+{}^iw_r{}^iP_r) \ , \tag{14}$$

where ${}^iP_r$ is the probability of a j-incrementing rotation about bond i given that a rotation about bond i is attempted. This probability is

$${}^iP_r=S_3+P_i(t)\frac{{}^i\tau_{g^-}}{{}^i\tau_{t^-}}=S_3+P_i(t)\frac{2\sigma}{1+\sigma'} \ . \tag{15}$$

Substituting Eq. (15) into Eq. (14) yields

$$Q=S_3+\frac{1}{Z}\frac{2\sigma}{1+\sigma'}\sum_{i=2}^{n-1}P_i(t){}^iw_r \ . \tag{16}$$

The essence of the timing scheme can be appreciated by considering the following approximation: Rotational weights are often small compared to S_3. When they are, $Q\approx S_3$, $Z\approx n-2$, and Eq. (13) reduces to

$$T\approx\frac{\tau_3}{n-2}j \ . \tag{17}$$

In this case, because rotational weights are negligible, nearly all jumps are three-bond jumps and j is approximately the number of three-bond jumps. The term $\tau_3/(n-2)$ is the average time for a three-bond jump to occur somewhere on the chain. The incorporation of S_3, Z, and Q in Eq. (13) takes care of the general case in which rotations are not infrequent. We used Eq. (13) to calculate the time for end-to-end contact.

III. SIMULATIONS

Three cases are treated in the Monte Carlo simulations: (1) intramolecular end-to-end contact in n-alkanes, (2) intramolecular fluorescence quenching in an end-labeled chain,[12] and (3) intramolecular electron exchange between naphthyl groups connected by an alkane chain.[17-22] In each case, a cutoff distance for contact, the time τ_3 for a three-bond jump, and the various rotational jump times ${}^i\tau_{g^-}$ must be specified.

It will be demonstrated that if most rotations are

slower than three-bond jumps, a change in the three-bond jump time does not have much effect on the rate of end-to-end contact. Even in unsubstituted n-alkanes, for which rotations are faster than in any other system which we consider, the dependence of the contact rate on the three-bond jump time is weak. Lyerla *et al.*[23] suggested that in the interior of an n-alkane chain, local bond rearrangements proceed with a correlation time of about 75 ps. In the n-alkane simulations we used 75 ps as the time τ_3 required for a *successful* three-bond jump. Thus, we did not consider the true connection between a correlation time for a three-bond jump and the jump time itself as discussed by Jones and Stockmayer,[24] because of the small effect produced by changes in τ_3. In the other two simulations, the large terminal substituents slow down the rotations of the chain ends, making the value chosen for τ_3 even less crucial. In those simulations, we let τ_3 equal 100 ps because an increase in τ_3 makes the simulation program more efficient.

To obtain estimates for the rotational jump times, we developed a simple scheme for deconvoluting carbon-13 spin–lattice relaxation times.[25] Spin–lattice relaxation times (T_1) in alkanes are simply related to the effective correlation time for reorientation of the C–H vectors at each carbon-13 nucleus.[23,26–28] We have argued that subtraction of the inverse correlation times for carbons i and $i+1$ yields an inverse correlation time ${}^i\tau_r^{-1}$ which characterizes the rate of rotation about bond i.[25] The method works best for methyl group rotation[23,26] and may be only a crude approximation for rotation about the second and third bonds, because the differing geometrical consequences of rotation about a particular C–C bond to the relaxation of the various C–H vectors in the rotating end group are ignored. From T_1 values for various alkanes in the literature,[23,25,26,29–31] ${}^2\tau_r$ at 38 °C is calculated to be approximately equal to 33 ps.

Such values are, however, effective rotational correlation times and not jump times for a 120° rotation. The conversion to a jump time is made by following Woessner.[32] He showed that if τ_c is the rotational correlation time for a bond that has three *equally* accessible rotational isomeric states, the jump time between the states is $\frac{3}{2}\tau_c$. Although the three states in alkanes (t, g^+, and g^-) are not equally accessible, we suggest that the average jump time is related to the effective rotational correlation time ${}^i\tau_r$ by

$$\langle {}^i\tau_{\text{jump}}\rangle = \tfrac{3}{2}\,{}^i\tau_r \,. \tag{18}$$

$\langle {}^i\tau_{\text{jump}}\rangle^{-1}$ is taken to be weighted average of inverse jump times for all types of rotation ($g^+ \rightarrow t$, $g^+ \rightarrow g^-$, $t \rightarrow g^+$, etc.):

$$\frac{1}{\langle {}^i\tau_{\text{jump}}\rangle} = \frac{2P_i(g^+)}{{}^i\tau_{g^+\rightarrow g^-}} + \frac{2P_i(g^+)}{{}^i\tau_{g^+\rightarrow t}} + \frac{2P_i(t)}{{}^i\tau_{t\rightarrow g^+}} \,, \tag{19}$$

where the factors of 2 are to include analogous terms for the g^- state. Ignoring the effects of g^+g^- sequences, approximate values of the required terms are

$$P_i(g^+) \approx \frac{\sigma}{1+2\sigma} \,, \tag{20}$$

$$P_i(t) \approx \frac{1}{1+2\sigma} \,, \tag{21}$$

$${}^i\tau_{t\rightarrow g^+} \approx {}^i\tau_{g^+\rightarrow t}/\sigma \,, \tag{22}$$

$${}^i\tau_{g^+\rightarrow g^-} \approx {}^i\tau_{g^+\rightarrow t}/\sigma' \,, \tag{23}$$

where $\sigma = \exp(-500/RT)$ and $\sigma' = \exp[-(V_{gg} - V_{gt})/RT]$ as discussed earlier.

A. Alkane simulation

The cutoff distance for chain end contact is taken to be the sum of the radii of the two terminal methyl groups for which a value of 3.5 Å was calculated from van der Waals increments.[33] Two cases were considered for rotational jumps out of a g state. In one, the jump times for rotation from g to t were taken to be equal to those for rotation from g^+ to g^- (i.e., $\sigma' = 1$). Then, with ${}^2\tau_r = 33$ ps at 38 °C one may use Eqs. (18)–(23) to calculate ${}^2\tau_{g^+\rightarrow g^-} = {}^2\tau_{g^+\rightarrow t} = 70$ ps or ${}^2\tau_{g\rightarrow} = 35$ ps. Because of the possible high barrier between g^+ and g^- compared with that between g^+ and t, this assumption of equal jump times may be unrealistic. In order to understand the magnitude of the error which may have been introduced by the assumption, we also ran alkane simulations for the extreme case in which rotations from g^+ to g^- were forbidden. In this second case ($\sigma' = 0$), use of Eqs. (18)–(23) gives ${}^2\tau_{g\rightarrow t} = {}^2\tau_{g\rightarrow} = 46.5$ ps.

Next, ${}^3\tau_{g\rightarrow t}$, ${}^4\tau_{g\rightarrow t}$, etc. were estimated from the following simple hydrodynamics: If one assumes that beads representing the methylene groups of an alkane chain are hydrodynamically independent, then the friction coefficient for the rotation of a terminal chain group about bond i is

$$\rho_i = \text{const} \sum_{k=1}^{i-1} r_k g_k^2 \,, \tag{24}$$

where k specifies the bead number with respect to the nearer end of the chain, r_k is the radius of bead k, and g_k is the perpendicular distance from bead k to the axis of rotation. The quantity ${}^i\tau_{g\rightarrow}$ is expected to be proportional to ρ_i. Equation (24) involves the implicit assumption that the remainder of the chain does not rotate. Strictly speaking, it is the *relative* rotational motion of the two chain segments on either side of bond i which should be considered but this was not done despite the fact that calculation of an approximate frictional constant ρ_{rel} for relative rotational motion is not difficult. The difference between ρ_{rel} and ρ_i of Eq. (24) is small for rotation about bonds near the end of the chain, and ρ_{rel} is never less than half the corresponding ρ_i value.

In applying Eq. (24) to alkanes, we calculated ρ_i for every possible conformation of a rotating end group, multiplied each ρ_i by an appropriate statistical weight, and computed an average value $\langle\rho_i\rangle$. The results are given in Table I. Values of ${}^i\tau_{g\rightarrow}$ for $i > 2$ were calculated by dividing ${}^2\tau_{g\rightarrow}$ by $\langle\rho_2\rangle/\langle\rho_i\rangle$. As shown in Table I, $\langle\rho_i\rangle$ is very large by the sixth bond, which means that rotations about bonds 7 and beyond (when they exist; e.g., they do not exist for C_{10} or C_{12}) are expected to occur at an insignificant rate. We did not allow rotations about bonds with $i \geq 7$.

TABLE I. Rotational friction coefficients for rotation about a bond in n-alkanes (units of ρ are Å^3).

Bond (i)	$\langle\rho_i\rangle$	$\langle\rho_2\rangle/\langle\rho_i\rangle$
2	3.66	1.000
3	10.38	0.353
4	23.96	0.153
5	46.16	0.079
6	77.69	0.047

A representative semilog plot of the number of surviving chains versus time which results from a simulation is given in Fig. 3. The decay is not detectably different from exponential either in the case of n-alkanes or in the intramolecular fluorescence quenching simulations which are discussed next. Each decay curve was least-squares fit to yield an apparent first-order rate constant for intramolecular end-to-end contact. Results for a series of simulations for chains of from 10 to 20 carbons are given in Table II.

TABLE II. First-order rate constants for end-to-end contact in n-alkanes. Results of simulations at 38 °C with $\tau_3 = 75$ ps and an assumed contact separation of 3.5 Å.

n	$10^{-\xi}k(s^{-1})^a$	$10^{-8}k(s^{-1})^b$
10	10.09	6.17
12	7.31	5.43
14	5.23	5.15
16	4.37	4.60
18	3.56	3.64
20	3.24	2.59

[a] $g^+ \rightarrow g^-$ and $g^- \rightarrow t$ rotations occur with identical jump times ($\sigma' = 1$) and ${}^2\tau_{g^-} = 35$ ps.

[b] $g^+ \rightarrow g^-$ rotations are forbidden ($\sigma' = 0$) and ${}^2\tau_{g^-} = 46.5$ ps.

B. Intramolecular fluorescence quenching

In an earlier paper[12] we described the measurement of the rate of intramolecular fluorescence quenching in the following compound (hereafter referred to as ACQ):

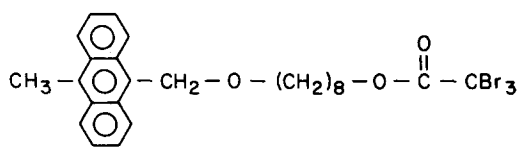

The rate of bimolecular fluorescence quenching of 9, 10-dimethylanthracene by various CBr_3 containing molecules was shown to be diffusion controlled, and hence the intramolecular fluorescence quenching rate is assumed to equal the rate of end-to-end contact. Here we extend the alkane simulations to the ACQ molecule. Some of the results of this simulation were previously communicated.[12]

We began by making two simplifying assumptions about the structure of ACQ. First, we treated the ether oxygen as if it were a methylene group. Second, we assumed that both the anthracene and the tribromoacetyl substituents could be approximated by spheres on either end of the chain. In short, ACQ is represented by an 11 bond chain. The first bond length is equal to the distance from the center of the anthracene to the first methylene carbon of the chain (3.5 Å). The nine internal bond lengths are assumed to be equal to the C–C distance in alkanes (1.53 Å). Finally, the last bond length

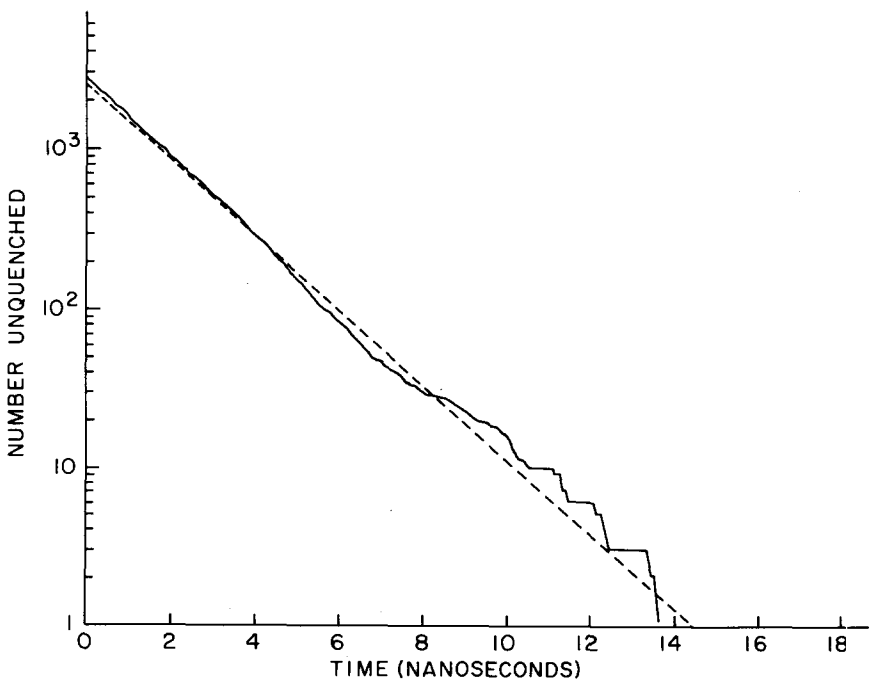

FIG. 3. Typical decay in the number of surving chains versus time. This decay is for ACQ intramolecular fluorescence quenching at 17 °C with $\tau_3 = 100$ ps and ${}^2\tau_{g^-} = 950$ ps.

TABLE III. Rotational friction coefficients for rotation about bonds in ACQ (units of ρ are Å^3).

	Anthracene end		Quencher end	
Bond (i)	$\langle\rho_i\rangle$	$\langle\rho_2\rangle/\langle\rho_i\rangle$	$\langle\rho_i\rangle$	$\langle\rho_2\rangle/\langle\rho_i\rangle$
2	27.92	1.000	28.53	1.000
3	30.08	0.928	66.22	0.431
4	67.28	0.415	87.01	0.328
5	90.13	0.310	135.0	0.211
6	144.8	0.193	172.5	0.165

is equal to the distance from the last carbon in the chain to the center of the tribromomethyl group (4.0 Å). The radii of the two terminal spheres were calculated by estimating the volumes of the substituents they represent using van der Waals increments.[33] Those radii are 3.0 and 3.5 Å for the anthracene and tribromo ester groups, respectively. The same RIS parameters are used for the ACQ chain as for the n-alkanes, and the cutoff distance for contact is taken to be equal to the sum of the radii of the two terminal spheres (6.5 Å).

In order to estimate rotational jump times about each bond in ACQ, we first computed relative friction coefficients using Eq. (24). Again, estimation of an effective friction constant involves a weighted average of friction coefficients for all conformations of the end group which is undergoing rotation. While in hydrocarbons the RIS energies needed for determination of the weights are known,[15] relative energies for the possible conformations about the bonds connecting the chain to the bulky terminal groups of ACQ are not known. Because of the large size of these groups, we assumed that the bonds adjacent to terminal bonds are *trans* to the rest of the chain. Effective friction constants computed as described above are presented in Table III. Multiplication of the value of ${}^2\tau_{g^-}$ equal to 35 ps by the ratio of $\langle\rho_2\rangle$ for ACQ to $\langle\rho_2\rangle$ for an alkane yields approximate values of ${}^2\tau_{g^-}$ equal to 250 ps for both the anthracene and quencher ends of ACQ at 38 °C. Using this value of ${}^2\tau_{g^-}$ and the friction constants in Table III, ${}^i\tau_{g^-}$ was calculated for rotation about each bond. In ACQ simulations, we took the jump times for $g^+ \rightarrow g^-$ and $g^+ \rightarrow t$ rotations to be equal ($\sigma' = 1$).

As discussed earlier, the three-bond jump time (τ_3) is expected to be about 75 ps. To test the effect of varying this jump time, we simulated intramolecular fluorescence quenching at 38 °C and let τ_3 range from 33 to 132 ps. The results in Table IV show that virtually no change in the rate of end-to-end contact resulted. In all other ACQ simulations, a τ_3 value of 100 ps was used.

TABLE IV. Intramolecular fluorescence quenching simulation at 38 °C. ${}^2\tau_{g^-}$ is constant at 250 ps while τ_3 varies.

τ_3	$10^{-8}\,k(s^{-1})$
33	9.14
66	9.26
132	9.40

TABLE V. Comparison of ACQ quenching simulations with experimental data.

	Experiment	Simulation
T (°C)	$10^{-8}k_c(s^{-1})$	$10^{-8}k_s(s^{-1})$
20	17.1	6.0
10	13.3	4.6
0	12.3	3.0
−10	9.2	1.9
−20	7.5	1.4
−30	5.6	0.91
	E_a = 3 kcal/mol	E_a = 5.5 kcal/mol

To extend the 38 °C simulation to other temperatures, the temperature dependence of the dynamical parameters is required. As stated above, variations in the three-bond jump time do not appear to affect the rate of end-to-end contact. Thus, τ_3 was fixed at 100 ps in the temperature-dependence simulations. To estimate the activation energy for rotation about internal bonds, we turned to carbon-13 spin lattice relaxation times (T_1) in 10-methylnonadecane for which T_1's have been measured as a function of temperature.[26] We used the T_1 values to estimate correlation times for rotation about bonds 2, 3, 4, and 5 at several temperatures.[25] The activation energy for rotation about each of these bonds was found to be 5 kcal/mol. Because the length of the rotating group did not appear to affect the activation energy, we assumed that the 5 kcal value applies to rotation about all internal C–C bonds in ACQ. Again, we have ignored the different rotational characteristics of the bonds to the ether oxygen. Figure 3 presents a representative decay curve from the ACQ simulations and rate constants are given as a function of temperature in Table V.

C. Intramolecular electron exchange

Szwarc and his co-workers have reported[17–22] the experimental determination of electron exchange rates in naphthyl–$(CH_2)_n$–naphthyl, where n varied from 3 to 20. Here we present a Monte Carlo simulation of those exchange rates. Again three types of parameters (cutoff distance, rotational jump times, and three-bond jump time) are required. Shimada and Szwarc[21,22] estimated the distance at which rapid electron transfer took place to be 7 to 9 Å. We have used both 7 and 8 Å as cutoff distances in two separate simulations. The rotational jump times were calculated in a manner exactly analogous to that used in the ACQ simulations. The ρ_i's are given in Table VI. By comparison to alkanes at 38 °C and assuming a 5 kcal activation energy, ${}^2\tau_{g^-}$ at 30 °C is found to be approximately 185 ps. Again, we used τ_3 equal to 100 ps.

In the case of intramolecular fluorescence quenching, the quenching was irreversible. In contrast, electron exchanges are reversible. The desired time constant is the round-trip time or the time it takes for a chain in a contacting conformation to return to a contacting conformation. Thus, in the electron exchange simulation

TABLE VI. Rotational friction coefficients for rotation about a bond in naphthyl–$(CH_2)_n$–naphthyl (units of ρ are Å^3).

Bond (i)	$\langle\rho_i\rangle$	$\langle\rho_2\rangle/\langle\rho_i\rangle$
2	19.35	1.00
3	55.27	0.35
4	74.41	0.26
5	129.0	0.15
6	175.9	0.11

we again use RIS statistics to choose an initial conformation, but this time allow it to evolve until the ends have come into contact twice. The elapsed time between the two contacts is the round-trip time. When the two ends are in contact, the electron can be rapidly interchanged and the net probability that an electron exchange has taken place by the time the ends separate is one half.[21] Therefore, the rate constant for electron exchange is assumed to be one half of the rate constant for the round-trip process.

The simulations for 30 °C are in Table VII. Even at the smaller cutoff distance of 7 Å, the simulation rate constants are 30 times larger than the experimental values. The chain length dependence of the rate is, however, reproduced fairly well.[34]

D. Discussion

To a good approximation, as noticed by Shimada and Szwarc,[21] the experimental electron exchange rate constants (see Table VII) fall off with chain length according to $n^{-3/2}$, where n is the number of carbons in the chain.[34] This same behavior is noticed in the simulation rate constants for the electron exchange. An $n^{-1.55}$ falloff is also observed in the alkane end-to-end contact simulations of Table II but only for the case in which the jump time for a g^+ to g^- rotation is taken to be equal to that for a g^+ to t rotation. If, as in the last column of Table II, g^+ to g^- rotations are forbidden, the falloff is less steep than $n^{-3/2}$. This latter assumption is thought to be more realistic than the equal jump time assumption. Nevertheless, over the chain length range investigated, all simulations exhibit a monotonic decrease of rate constant with increasing chain length. The simulations of equilibrium chain conformational distributions of Sisido and Shimada[35] appear to establish that this monotonic decrease of rate constant with n reflects the decreasing probability that as n increases the ends of a chain will be separated by no more than the cutoff distance.

Comparison of the magnitudes of the experimental rate constants of Tables V and VII with the corresponding values from the simulations provides a direct test of the many assumptions which the simulation model contains. In Table V the simulation rate constant at 20 °C is less than the experimental rate constant by a factor of about 3 and this ratio increases to about 6 by −30 °C. Several possibilities for rate constant discrepancies are present in the assumptions which govern the simulations: (1) Long-range excluded volume effects are ignored; (2) possible steric or orientational requirements for end-to-end interaction (quenching or electron transfer) are ignored; (3) the ether linkage of the ACQ chain is treated as a hydrocarbon linkage; (4) the chain backbone is confined to a tetrahedral lattice; and (5) approximate procedures are used to calculate the jump times required in the simulation.

Assumptions (1) and (2) above should result in simulation rate constants that are larger than the experimental values. Assumption (1) results in the counting of some physically forbidden conformations as contributors to the set of end-to-end contact conformations. On the other hand, assumptions (3) and (4) should result in simulation rates that are slower than experimental rates, as is observed in the fluorescence quenching case (Table V). Rotations about the C–O bonds of an ether linkage are generally thought to be faster than are those about the C–C bonds of a hydrocarbon. Perhaps the most directly relevant example is provided by the intramolecular electron exchange results of Shimada *et al.*,[20] where substitution of a $-(CH_2CH_2O)_mCH_2CH_2-$ chain for a hydrocarbon chain with the same number of skeleton atoms raised the values of the electron exchange rate by a factor of about 3.

The confinement of the chain to a tetrahedral lattice freezes out angle variations and surely represents a serious deficiency of the simulation. Recently, there have been several Brownian or molecular dynamics studies[36,37] of chains not confined to lattices and allowed to change bond angles or torsional angles or both. Also, a new theory of conformational transitions has been formulated by Skolnick and Helfand.[38] These developments suggest strongly that the dominant local process is not accurately describable by any crankshaft model; rather, the reaction coordinate involves passage over only a

TABLE VII. Comparison of electron exchange simulations with experimental data.

	Experimental[a]		7 Å Cutoff		8 Å Cutoff	
Carbon links n	$10^{-8}\,k(s^{-1})$	Relative to $n=12$	$10^{-8}\,k(s^{-1})$	Relative to $n=12$	$10^{-8}\,k(s^{-1})$	Relative to $n=12$
8	0.43	1.23	11.7	1.54	15.4	1.72
10	0.39	1.11	8.62	1.13	12.4	1.39
12	0.35	1	7.61	1	8.93	1
16	0.16	0.46	4.58	0.60	5.86	0.66
20	0.10	0.29	3.48	0.46	3.96	0.44

[a]Reference 21, but see Ref. 34.

single barrier, though it is basically still a localized mode. Perhaps even more important for the present study, many noncontacting RIS conformations can be brought into end-to-end contact by the cumulative effect of small variations of bond angles or torsional angles without the necessity of crossing even a single barrier. Of course, contacting RIS conformations can be distorted into noncontacting conformations by angle variations as well, but since the contacting conformations are a small fraction of all RIS conformations,[35] angle variability should provide for a net increase in contact rate. The effects of torsional angle variability on the end-to-end distance of short RIS chains have been studied by Cook and Moon[39] and by Mansfield.[40] Cook and Moon find that for a ten-bond chain, a 10° rms deviation in torsional angles produces a substantial rms deviation in the end-to-end distance for a single RIS conformation.

Angle variability allows for the possibility of the diffusion together of the two chain ends during a time period when the nominal RIS conformation does not change. The temperature dependence of this diffusion should be governed mainly by that of the viscosity. The experimental ACQ rate constants of Table V are characterized by an activation energy of about 3 kcal/mol, not much greater than the 2.5 kcal/mol activation energy for viscous flow in the methylcyclohexane solvent which was used. The low experimental activation energy compared to the 5.5 kcal/mol activation energy which characterizes the simulation temperature dependence (Table V) may, together with the larger experimental rate constants, point to the importance of angle variability and end-to-end diffusion in the experimental results.

Alternatively, one may question the validity of the 5 kcal/mol activation energy for a rotational jump which was built into the simulation and which governs the resulting activation energy for end-to-end contact. The 5 kcal/mol activation energy originates in the temperature dependence of the NMR difference correlation times which we have assigned to rotational jumps.[25] It appears to be a reasonable value in that if a rotational jump is interpreted via the Kramers theory,[41] the overall activation energy for the jump is the sum of the barrier height and the activation energy for the reciprocal viscosity. The 3 kcal/mol barrier height for a $g \rightarrow t$ rotation added to the typical 2 kcal/mol activation energy for viscous flow in n-alkanes corresponds nicely to the 5 kcal/mol activation energy seen in the differences of reciprocal correlation times. However, it appears from the recent work of Montgomery *et al.*[42] that Kramers theory may not be strictly applicable to the $g \rightleftharpoons t$ transitions of hydrocarbons in nonviscous solvents.

It is difficult to assess the accuracy of the jump times used in the simulations. As discussed earlier, the three-bond jump time is not a crucial parameter, but any errors in the rotational jump times will lead to errors of comparable magnitude in the simulation rate constants. Here a key concern is that no explicit account was taken of differences in viscosity between the neat alkane and other liquids used in the ^{13}C relaxation studies[25] and the solvent systems used in the ACQ quenching and in the intramolecular electron transfer studies. Recall that the crucial time constant extracted from the ^{13}C NMR studies was the correlation time $^{2}\tau_r$ assigned to rotation about the second bond of an alkane chain. This time constant was not observed to have any clear dependence on solvent viscosity.[25] We attributed this to a more or less constant microviscosity for the small scale motions associated with rotations of a methyl group about the second bond of a chain. However, in the ACQ and electron transfer experiments, bulky end groups move through the solvent in all rotations which change the end-to-end distance. The jump times for these motions seem likely to depend on the macroscopic solution viscosity. Therefore, our procedure of using geometrically determined relative friction constants alone to extrapolate from the alkane case to the bulky-end-group situation is likely to be in error, but by an unknown amount. We intend to study intramolecular quenching in solvents of different viscosity in an attempt to gain some insight into this problem. It should also be pointed out that while we believe that torsional angle oscillations are probably important in increasing the measured ACQ quenching rates compared to the simulation rates, the oscillations make some contribution to the difference correlation times which we have attributed solely to rotational jumps. Thus, the correlation time treatment may underestimate the time required for a full rotational jump. However, harmonic components of the torsional oscillations do not contribute to the ^{13}C relaxation even though they cause variation in the end-to-end distance and thereby increase the end-to-end contact rate compared to that of the simulations in which only full rotational jumps are allowed.

The intramolecular electron exchange simulations result in discrepancies, when compared with experimental rate constants, that are opposite in sign to those observed in the ACQ case. In Table VII, the simulation rate constants are about 30 times larger than the experimental rate constants. With the exception of assumption (3), the five assumptions examined above for the ACQ case are still involved in the electron transfer simulations. Assumptions (1) and (4) should produce effects of the same magnitude in both the ACQ and electron transfer cases which leaves (2) and (5) as sources of the turnabout between experiment and simulation.

It may well be that much of the difference arises from viscosity effects which, as described above, are ignored in the simulations. The solvent used in measurement of the experimental rate constants of Table VII was HMPA (hexamethylphosphoramide).[21] The viscostiy of HMPA is about a factor of 5 higher than that for methylcyclohexane, the solvent in the ACQ studies. In the diffusion limit of the Kramers theory, the jump times are directly proportional to solution viscostiy. Additionally, the simulation rates may be too high because the "contact" radii of 7 and 8 Å used in the simulations is too large or because orientational effects which might be important in determining the probability of electron transfer were ignored. This latter possibility suggests itself in that the measured bimolecular rate constants for electron transfer between alkylnaphthalenes at 30 °C[21] appear to be about a factor of 2 slower than diffusion-controlled rate constants.

E. Summary and conclusions

We have described Monte Carlo simulations of the dynamics of end-to-end contact in alkane chains. End-to-end contact is found to obey first-order kinetics and the rate constants decrease approximately as $n^{-3/2}$, where n is the number of atoms in the chain. This approximate chain length dependence has been observed experimentally in the electron transfer experiments of Shimada and Szwarc.[21] The magnitude of the rate constants derived from a simulation of the intramolecular fluorescence quenching results of Nairn *et al.*[12] agrees with experiment to within a factor of 3 to 6 depending on temperature. This assignment is satisfying in that there are no adjustable parameters in the simulation. Of the many approximations required in the simulations, confinement of the chains to a diamond lattice is thought to be most serious in that torsional angle variations in real alkane chains may well make a sizeable contribution to the actual rate of end-to-end contact.

ACKNOWLEDGMENTS

The authors are pleased to acknowledge many helpful conversations on chain conformational dynamics with Dr. Waldemar Silberszyc.

[1]L. Ruzicka, W. Brugger, M. Pfeiffer, H. Schinz, and M. Stoll, Helv. Chim. Acta **9**, 499 (1926).
[2]M. Stoll and A. Rouvé, Helv. Chim. Acta **18**, 1087 (1935).
[3]K. Ziegler and R. Aurnhammer, Justus Liebigs Ann. Chem. **513**, 43 (1934).
[4]V. Prelog, J. Chem. Soc. **1950**, 420.
[5]J. C. Wang and N. Davidson, J. Mol. Biol. **19**, 469 (1966).
[6]H. Jacobson and W. H. Stockmayer, J. Chem. Phys. **18**, 1600 (1950).
[7]M. A. D. Fluendy, Trans. Faraday Soc. **59**, 1681 (1963).
[8]M. Fixman and R. Alben, J. Chem. Phys. **58**, 1553 (1973).
[9]H. Morawetz and N. Goodman, Macromolecules **3**, 699 (1970).
[10]M. Sisido, Macromolecules **4**, 737 (1971).
[11]P. J. Flory, U. W. Suter, and M. Mutter, J. Am. Chem. Soc. **98**, 5733 (1976).
[12]J. A. Nairn, C. L. Braun, P. Caluwe, and M. Szwarc, Chem. Phys. Lett. **54**, 469 (1978).
[13]P. J. Flory, *Statistical Mechanics of Chain Molecules* (Interscience, New York, 1969).
[14]M. A. Winnik, Acc. Chem. Res. **10**, 173 (1977).
[15]P. J. Flory, Science **188**, 1268 (1975).
[16]L. Monnerie and F. Gény, J. Chim. Phys. Phys.-Chim. Biol. **66**, 1691 (1969); **66**, 1698 (1969); F. Gény and L. Monnerie, *ibid.* **66**, 1708 (1969); **66**, 1872 (1969); F. Gény and L. Monnerie, J. Polym. Sci. Part C **30**, 93 (1970).
[17]H. D. Connor, K. Shimada, and M. Szwarc, Chem. Phys. Lett. **14**, 402 (1972).
[18]K. Shimada, G. Moshuk, H. D. Connor, P. Caluwe, and M. Szwarc, Chem. Phys. Lett. **14**, 396 (1972).
[19]K. Shimada and M. Szwarc, J. Am. Chem. Soc. **97**, 3321 (1975).
[20]K. Shimada, Y. Shimozato, and M. Szwarc, J. Am. Chem. Soc. **97**, 5834 (1975).
[21]K. Shimada and M. Szwarc, J. Am. Chem. Soc. **97**, 3313 (1975).
[22]K. Shimada and M. Szwarc, Chem. Phys. Lett. **28**, 540 (1974).
[23]J. R. Lyerla, Jr., H. M. McIntyre, and D. A. Torchia, Macromolecules **7**, 11 (1974).
[24]A. A. Jones and W. H. Stockmayer, J. Polym. Sci. Polym. Phys. Ed. **15**, 847 (1977).
[25]J. A. Nairn and C. L. Braun, Chem. Phys. Lett. **52**, 385 (1977).
[26]J. R. Lyerla, Jr. and T. T. Horikawa, J. Phys. Chem. **80**, 1106 (1976).
[27]K. F. Kuhlmann, D. M. Grant, and R. K. Harris, J. Chem. Phys. **52**, 3439 (1970).
[28]A. Abragam, *The Principles of Nuclear Magnetism* (Oxford University, London, 1961).
[29]G. C. Levy, R. A. Komoroski, and J. A. Halstead, J. Am. Chem. Soc. **96**, 5456 (1974).
[30]J. R. Lyerla, Jr. and G. C. Levy, *Topics in Carbon-13 NMR Spectroscopy*, edited by G. C. Levy (Wiley, New York, 1974), p. 79.
[31]D. Doddrell and A. Allerhand, J. Am. Chem. Soc. **93**, 1558 (1971).
[32]D. E. Woessner, J. Chem. Phys. **36**, 1 (1962).
[33]J. T. Edward, J. Chem. Educ. 47, 261 (1970).
[34]The 30 °C experimental rate constants (Table VII) do not happen to follow closely the approximate $n^{-3/2}$ behavior demonstrated by the experimental rate constants at −15, 0, and +15 °C (see Ref. 21).
[35]M. Sisido and K. Shimada, J. Am. Chem. Soc. **99**, 7785 (1977); M. Sisido and K. Shimada, Macromolecules **12**, 790 (1979).
[36]E. Helfand, Z. R. Wasserman, and T. A. Weber, Macromolecules **13**, 526 (1980), and references given therein.
[37]Yu. Ya. Gotlib, N. K. Balabaev, A. A. Darinskii, and I. M. Neelov, Macromolecules **13**, 602 (1980).
[38]J. Skolnick and E. Helfand, J. Chem. Phys. **72**, 5489 (1980).
[39]R. Cook and M. Moon, Macromolecules **11**, 1054 (1978).
[40]M. L. Mansfield, J. Chem. Phys. **72**, 3923 (1980).
[41]H. A. Kramers, Physica (Utrecht) **7**, 284 (1940).
[42]J. A. Montgomery, Jr., D. Chandler, and B. J. Berne, J. Chem. Phys. **70**, 4056 (1979).